

# Work fluctuations for a harmonically confined Active Ornstein-Uhlenbeck Particle

Massimiliano Semeraro,<sup>1</sup> Giuseppe Gonnella,<sup>1</sup> Antonio Suma,<sup>1</sup> and Marco Zamparò<sup>1</sup>

<sup>1</sup>*Dipartimento Interateneo di Fisica, Università degli Studi di Bari and INFN,  
Sezione di Bari, via Amendola 173, Bari, I-70126, Italy*

(Dated: February 27, 2023)

We study the active work fluctuations of an active Ornstein-Uhlenbeck particle in the presence of a confining harmonic potential. We tackle the problem analytically both for stationary and generic uncorrelated initial states. Our results show that harmonic confinement can induce singularities in the active work rate function, with linear stretches at large positive and negative active work, at sufficiently large active and harmonic force constants. These singularities originate from big jumps in the displacement and in the active force, occurring at the initial or ending points of trajectories and marking the relevance of boundary terms in this problem.

Large deviation theory has a profound impact in statistical physics [1, 2]. In non-equilibrium systems, where probability measures on configuration spaces are not naturally available, it provides an analogous of the usual equilibrium free-energy description. Given an extensive physical observable  $W_\tau$  computed by cumulating a large number  $\tau$  of microscopic events, if a large deviation principle holds, then the asymptotics of the probability distribution  $P(W_\tau/\tau = w)$  can be characterized by the rate function  $I(w) = -\lim_{\tau \rightarrow \infty} \frac{1}{\tau} \ln P(W_\tau/\tau = w)$  [3, 4]. The probability distribution is dominated by small fluctuations around the minimum of  $I$ , which in this sense plays a role similar to a free-energy.

Singularities in rate functions can be seen as the hallmarks of phase transitions [2, 5]. They appear in different contexts, such as in studies of heat exchanges, diffusive transport, and entropy production [6–18], and in some cases have been interpreted as due to a condensation mechanism [19–27]. If  $\tau$  is a time interval, the rate function can provide a generalized thermodynamic description based on the counting of trajectories, and the singularity would correspond to a phase separation in trajectory space [28–30].

Active matter systems [31], with their inherent nonequilibrium character, offer a new field for applications of large deviation theory and investigations on dynamical phase transitions. In these systems, available energy sources are locally employed to produce spontaneous motion or work on the environment. They are characterized by a surprisingly rich phenomenology, including new important phenomena like motility induced phase separation (MIPS) [32] or spontaneous flow [31], and also concerning fluctuation properties [33–42].

A crucial quantity for the description of dynamical transitions in active matter models is the active work, defined as the time-average of the power of the propulsion force. In dilute systems of active Brownian particles, the active work rate function was shown to be singular [34], with a linear tail associated to trajectories where a particle does not diffuse freely but is dragged by a cluster moving oppositely to its propulsion force. Successive studies have revealed a very rich structure for the phase

diagram in trajectory space [43–45]. Rate functions for quantities analogous to active work were investigated in experiments of polar beads embedded in two-dimensional granular layers [46] and idealized Maxwell-Lorentz granular systems [47].

Most of the aforementioned results were based on numerical, although sophisticated, studies of interacting particle models. Rigorous analysis of simpler models can help to elucidate the role of self-propulsion in dynamical transitions. In this Letter we consider a single active Ornstein-Uhlenbeck particle (AOUP) [48–57] and investigate analytically the active work fluctuations in the presence of a confining harmonic potential. AOUP systems share many of the relevant properties of other interacting active particle models, including MIPS. Restricting to one particle description, a confining potential can mimic the trapping created by other particles at finite densities [48, 58, 59]. We will show that, differently from the case of a free AOUP [60], harmonic confinement can induce singularities in the active work rate function, with linear stretches at large positive and negative active work. These singularities are found both for stationary and generic uncorrelated initial states at sufficiently large active and harmonic force constants. They originate from big jumps in the displacement and in the active force, occurring at the initial or ending points of trajectories and marking the relevance of boundary terms in this problem.

The unidimensional active particle model that we study is defined via the Ornstein-Uhlenbeck process

$$\begin{cases} \gamma \dot{r}(t) = a(t) - kr(t) + \sqrt{2\gamma k_B T} \xi(t) \\ \dot{a}(t) = -\nu a(t) + F\sqrt{2\nu} \eta(t), \end{cases} \quad (1)$$

where  $r(t)$  is the position of a unit-mass particle in a harmonic potential of elastic constant  $k$ ,  $a(t)$  represents a self-propulsion force with amplitude  $F$  and decay rate  $\nu$ ,  $\gamma$  and  $T$  are the friction coefficient and the bath temperature, and  $\xi(t)$  and  $\eta(t)$  are two independent zero-mean and unit-variance white noises. One has  $\nu \equiv k_B T / \gamma d^2$  with  $d$  being a length proportional to the particle's diameter and related to the ratio between the rotational and translational diffusion coefficients [61]. We will vary the

dimensional elastic constant  $\kappa \equiv \frac{kd^2}{k_B T}$  and the *Péclet number*  $\text{Pe} \equiv \frac{Fd}{k_B T}$ , which quantify the strength of the potential and of the active force with respect to thermal fluctuations [61, 62]. Without loss of generality, in the following we set  $\gamma = 1$ ,  $k_B T = 1$ , and  $d = 1$ .

In order to analyze the dynamical behavior of the AOUP model (1), we examine the probability distribution of the *active work*  $W_\tau$  defined by the formula [63]

$$W_\tau \equiv \int_0^\tau a(t) \dot{r}(t) dt.$$

The active work represents a measure of how efficiently self-propulsion is converted into directed motion. Our goal is to evaluate the rate function  $I(w) = -\lim_{\tau \uparrow \infty} \frac{1}{\tau} \ln P(W_\tau/\tau = w)$ . The probability distribution  $P(W_\tau/\tau = w)$  can be expressed by the path integral

$$P(W_\tau/\tau = w) = \int \delta(W_\tau - w\tau) \mathcal{P}_\tau \mathcal{D}r \mathcal{D}a$$

with path probability

$$\mathcal{P}_\tau \propto \exp \left\{ -\frac{1}{2} (r(0) \ a(0)) \Sigma_0^{-1} \begin{pmatrix} r(0) \\ a(0) \end{pmatrix} \right\} \times \exp \left\{ -\int_0^\tau \left( \frac{[\dot{r}(t) - a(t) + \kappa r(t)]^2}{4} + \frac{[\dot{a}(t) + a(t)]^2}{4\text{Pe}^2} \right) dt \right\}.$$

The probability  $\mathcal{P}_\tau$  combines the distribution of the initial values  $r(0)$  and  $a(0)$  with the Onsager-Machlup weight for the trajectory [64]. We have chosen Gaussian initial data with mean zero and joint covariance matrix  $\Sigma_0$ . In particular, we focus on a non-stationary uncorrelated initial condition with standard deviations  $\sigma_r$  for  $r(0)$  and  $\sigma_a$  for  $a(0)$ , and on the stationary case given by [65]

$$\Sigma_0 = \begin{pmatrix} \frac{1+\kappa+\text{Pe}^2}{\kappa(1+\kappa)} & \frac{\text{Pe}^2}{1+\kappa} \\ \frac{\text{Pe}^2}{1+\kappa} & \text{Pe}^2 \end{pmatrix}. \quad (2)$$

An operative definition of the rate function  $I$  requires to first look at a discrete-time problem with time step  $\epsilon$ , and then to consider the continuum limit  $\epsilon \downarrow 0$ . In fact, we compute  $I$  by means of the double limit  $I(w) = -\lim_{\epsilon \downarrow 0} \lim_{N \uparrow \infty} \frac{1}{N\epsilon} \ln P(W_N/N\epsilon = w)$ , where  $W_N \equiv \frac{1}{2} \sum_{n=1}^N (a_n + a_{n-1})(r_n - r_{n-1})$  with  $r_n \equiv r(n\epsilon)$  and  $a_n \equiv a(n\epsilon)$  is the discretized active work at time  $N\epsilon$ . The discrete-time problem is tackled by computing the asymptotic cumulant generating function  $\frac{1}{N} \ln \langle e^{\lambda W_N} \rangle$  of  $W_N$  at large  $N$ . The Legendre-Fenchel transform of  $\lim_{N \uparrow \infty} \frac{1}{N} \ln \langle e^{\lambda W_N} \rangle$  with respect to the additional variable  $\lambda$  is expected to be the discrete-time rate function  $J(w) = -\lim_{N \uparrow \infty} \frac{1}{N} \ln P(W_N/N = w)$ . We have  $I(w) = \lim_{\epsilon \downarrow 0} \frac{J(\epsilon w)}{\epsilon}$ .

At small  $\epsilon$ , the trajectory  $\{(r_0, a_0), \dots, (r_N, a_N)\}$  is distributed according to a multivariate Gaussian law with mean zero and covariance matrix  $\Sigma_N$  [66]. Regarding

$W_N$  as a quadratic functional of  $\{(r_0, a_0), \dots, (r_N, a_N)\}$  with coefficient matrix  $\frac{1}{2} \mathbf{M}_N$ , a standard Gaussian integral gives

$$\ln \langle e^{\lambda W_N} \rangle = -\frac{1}{2} \ln \det(\Sigma_N^{-1} - \lambda \mathbf{M}_N) - N \ln(2\epsilon \text{Pe}) - \frac{1}{2} \ln \det \Sigma_0$$

if  $\Sigma_N^{-1} - \lambda \mathbf{M}_N$  is positive definite and  $\ln \langle e^{\lambda W_N} \rangle = +\infty$  otherwise.  $\Sigma_N^{-1} - \lambda \mathbf{M}_N$  is the block tridiagonal matrix

$$\Sigma_N^{-1} - \lambda \mathbf{M}_N = \begin{pmatrix} L & V^\top & & & \\ V & U & \ddots & & \\ & \ddots & \ddots & \ddots & \\ & & & U & V^\top \\ & & & V & R \end{pmatrix} \quad (3)$$

with  $2 \times 2$  blocks  $L \equiv \Sigma_0^{-1} + S^\top D^{-2} S + \lambda E_+$ ,  $U \equiv D^{-2} + S^\top D^{-2} S$ ,  $R \equiv D^{-2} - \lambda E_+$ ,  $V \equiv -D^{-2} S - \lambda E_-$ ,  $S \equiv \begin{pmatrix} 1-\kappa\epsilon & \epsilon \\ 0 & 1-\epsilon \end{pmatrix}$ ,  $D \equiv \begin{pmatrix} \sqrt{2\epsilon} & 0 \\ 0 & \text{Pe}\sqrt{2\epsilon} \end{pmatrix}$ , and  $E_\pm \equiv \frac{1}{2} \begin{pmatrix} 0 & 1 \\ \pm 1 & 0 \end{pmatrix}$ . We observe that  $\Sigma_N^{-1} - \lambda \mathbf{M}_N$  differs from a perfect block tridiagonal Toeplitz matrix by the extreme diagonal blocks  $L$  containing  $\Sigma_0$  and  $R$ , which play a subtle but important role in determining positive definiteness. We denote by  $\mathbb{T}_N$  the block Toeplitz bulk matrix obtained from  $\Sigma_N^{-1} - \lambda \mathbf{M}_N$  by deleting all contour blocks.

Evaluating the limit  $\lim_{N \uparrow \infty} \frac{1}{N} \ln \langle e^{\lambda W_N} \rangle$  is a nontrivial task. For those values of  $\lambda$  that make  $\Sigma_N^{-1} - \lambda \mathbf{M}_N$  positive definite, the asymptotic cumulant generating function of  $W_N$  is only determined by the bulk matrix  $\mathbb{T}_N$ . In fact, the results of [67] for generic quadratic functionals based on Szegő theorem for block Toeplitz matrices [68] show that if  $\Sigma_N^{-1} - \lambda \mathbf{M}_N$  is positive definite in the large  $N$  limit, then

$$\begin{aligned} \lim_{N \uparrow \infty} \frac{1}{N} \ln \langle e^{\lambda W_N} \rangle &= \varphi(\lambda) \\ &\equiv -\frac{1}{4\pi} \int_0^{2\pi} \ln \det F_\lambda(\theta) d\theta - \ln(2\epsilon \text{Pe}) \end{aligned}$$

with  $F_\lambda(\theta) \equiv V e^{-i\theta} + U + V^\top e^{i\theta}$ . The Hermitian matrix function  $F_\lambda$  is the so-called *symbol* of  $\mathbb{T}_N$  [68].

For  $\Sigma_N^{-1} - \lambda \mathbf{M}_N$  being positive definite it is necessary and sufficient that both  $\mathbb{T}_N$  and its Schur complement

$$\mathbf{S}_N \equiv \begin{pmatrix} L - V^\top (\mathbb{T}_N^{-1})_{11} V & -V^\top (\mathbb{T}_N^{-1})_{1N} V^\top \\ -V (\mathbb{T}_N^{-1})_{N1} V & R - V (\mathbb{T}_N^{-1})_{NN} V^\top \end{pmatrix}$$

are positive definite,  $(\mathbb{T}_N^{-1})_{ij}$  being the  $2 \times 2$  block of  $\mathbb{T}_N^{-1}$  in the row  $i$  and column  $j$ . The extreme diagonal blocks  $L$  and  $R$  enter  $\mathbf{S}_N$  and thus come into play in establishing positive definiteness. The Toeplitz matrix  $\mathbb{T}_N$  is positive definite if its symbol  $F_\lambda$  has the same property [67]. This introduces a first constraint on  $\lambda$ ,

which defines the *primary domain*  $(\tilde{l}_-, \tilde{l}_+)$  of  $\varphi$ . It can be shown [67] that  $\lim_{N \uparrow \infty} S_N = \begin{pmatrix} \mathcal{L}_\lambda & 0 \\ 0 & \mathcal{R}_\lambda \end{pmatrix}$ ,  $\mathcal{L}_\lambda$  and  $\mathcal{R}_\lambda$  being  $2 \times 2$  symmetric matrices determined by  $L$ ,  $R$ , and  $F_\lambda$ , whose explicit expression in the limit  $\epsilon \downarrow 0$  is reported in [66]. Then, a second constraint on  $\lambda$  comes from the requirement that  $\mathcal{L}_\lambda$  and  $\mathcal{R}_\lambda$  are positive definite. Denoting by  $(l_-, l_+)$  the interval of  $\lambda$  for which both constraints are fulfilled, i.e. the *effective domain* of  $\varphi$ , we get  $\lim_{N \uparrow \infty} \frac{1}{N} \ln \langle e^{\lambda W_N} \rangle = \varphi(\lambda)$  for  $\lambda \in (l_-, l_+)$  and  $\lim_{N \uparrow \infty} \frac{1}{N} \ln \langle e^{\lambda W_N} \rangle = +\infty$  for  $\lambda \notin [l_-, l_+]$ . We have  $\tilde{l}_- \leq l_- < 0 < l_+ \leq \tilde{l}_+$ .

We are now in the position to compute the discrete-time rate function  $J$  as the Legendre-Fenchel transform of  $\varphi$ , that is  $J(w) = \sup_{\lambda \in (l_-, l_+)} \{w\lambda - \varphi(\lambda)\}$ . We stress that this way of computing the rate function  $J$ , although natural, cannot be justified by the classical Gärtner-Ellis theorem [3, 4] since in general  $\varphi$  is not steep at the boundary of the effective domain. In fact, the Gärtner-Ellis theorem requires that the derivative of  $\varphi$  diverges when the boundary points  $l_-$  and  $l_+$  are approached, but this fails when  $l_- > \tilde{l}_-$  or  $l_+ < \tilde{l}_+$ . The above formula for  $J$  can be demonstrated by means of a time-dependent change of probability measure [67]. From a mathematical point of view, the lack of steepness is the hallmark of a dynamical phase transition.

The last job is to take the continuum limit. Notice that  $\tilde{l}_\pm$ ,  $l_\pm$ , and  $\varphi(\lambda)$  depend on  $\epsilon$ . Cumbersome calculations summarized in [66] yield

$$I(w) = \lim_{\epsilon \downarrow 0} \frac{J(\epsilon w)}{\epsilon} = \sup_{\lambda \in (\lambda_-, \lambda_+)} \{w\lambda - \phi(\lambda)\} \quad (4)$$

with  $\lambda_\pm \equiv \lim_{\epsilon \downarrow 0} l_\pm$  and asymptotic cumulant generating function

$$\begin{aligned} \phi(\lambda) &\equiv \lim_{\epsilon \downarrow 0} \frac{\varphi(\lambda)}{\epsilon} \\ &= \frac{1 + \kappa}{2} - \frac{1}{2} \sqrt{(1 + \kappa)^2 - 4\text{Pe}^2 \lambda(1 + \lambda)}. \end{aligned} \quad (5)$$

The primary domain in the limit  $\epsilon \downarrow 0$  is found to be described by the compact formula

$$\tilde{\lambda}_\pm \equiv \lim_{\epsilon \downarrow 0} \tilde{l}_\pm = -\frac{1}{2} \pm \frac{1}{2} \sqrt{1 + \left(\frac{1 + \kappa}{\text{Pe}}\right)^2}. \quad (6)$$

An explicit formula for the boundary points  $\lambda_\pm$  of the effective domain in the continuum limit is not available.

According to Eq. (5), the asymptotic cumulant generating function  $\phi$  is steep on the primary domain  $(\tilde{\lambda}_-, \tilde{\lambda}_+)$  as  $\lim_{\lambda \downarrow \tilde{\lambda}_-} \phi'(\lambda) = -\infty$  and  $\lim_{\lambda \uparrow \tilde{\lambda}_+} \phi'(\lambda) = +\infty$ . On the contrary,  $w_- \equiv \phi'(\lambda_-) > -\infty$  if  $\lambda_- > \tilde{\lambda}_-$  and  $w_+ \equiv \phi'(\lambda_+) < +\infty$  if  $\lambda_+ < \tilde{\lambda}_+$ , so that  $\phi$  is not steep on the effective domain  $(\lambda_-, \lambda_+)$  when  $\lambda_- > \tilde{\lambda}_-$  or  $\lambda_+ < \tilde{\lambda}_+$ . The lack of steepness originates linear tails of the rate function  $I$  that begin at the singular points  $w_-$  and  $w_+$ .

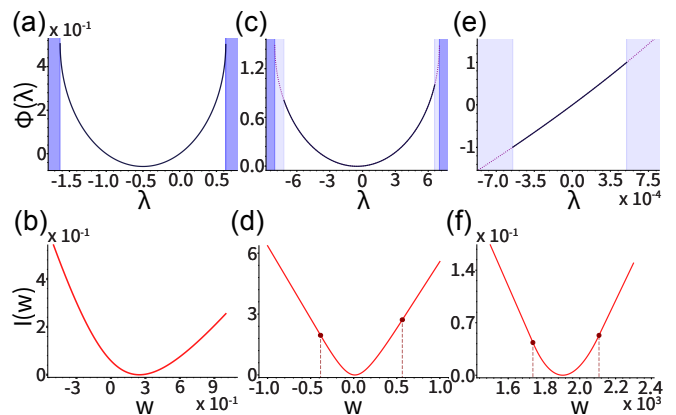


FIG. 1. Asymptotic cumulant generating function  $\phi(\lambda)$  and rate function  $I(w)$  under a concentrated non-stationary initial condition with  $\sigma_r \downarrow 0$  and  $\sigma_a \downarrow 0$  for  $\kappa = 0.01$  and  $\text{Pe} = 0.5$  in (a) and (b), under the stationary initial condition with  $\kappa = 2.0$  and  $\text{Pe} = 0.2$  in (c) and (d), and under the stationary initial condition with  $\kappa = 20.0$  and  $\text{Pe} = 200.0$  in (e) and (f). The dark and light blue areas in (a), (c), and (e) mark the regions outside the primary and effective domain, respectively. The dotted lines in (d) and (f) mark the beginning of the left linear tail at  $w_-$  and of the right one at  $w_+$ .

In fact, the supremum in Eq. (4) reads

$$I(w) = \begin{cases} \lambda_-(w - w_-) + i(w_-) & \text{if } w \leq w_-, \\ i(w) & \text{if } w_- < w < w_+, \\ \lambda_+(w - w_+) - i(w_+) & \text{if } w \geq w_+ \end{cases}$$

with  $i(w) \equiv \frac{\sqrt{1+(w/\text{Pe})^2} \sqrt{(1+\kappa)^2 + \text{Pe}^2 - 1 - \kappa - w}}{2}$ . Interestingly, the smooth function  $i$  is the rate function of the entropy production at stationarity [66], and as such satisfies the Gallavotti-Cohen symmetry  $i(-w) = i(w) + w$  at variance with  $I$ . The entropy production differs from the active work by local contributions of the initial and ending points of the trajectory [66], which prevent its rate function from exhibiting singularities at stationarity [66], a circumstance that boosts the interest in the active work.

Fig. 1 shows the functions  $\phi$  and  $I$ . Figs. 1(a) and 1(b) refer to the concentrated non-stationary initial condition  $\sigma_r \downarrow 0$  and  $\sigma_a \downarrow 0$ , for which the primary and the effective domain coincide. Figs. 1(c) and 1(d), and Figs. 1(e) and 1(f), correspond to stationary initial conditions with different parameters. At stationarity the rate function has a left linear tail, i.e.  $\lambda_- > \tilde{\lambda}_-$ , for  $\text{Pe} \sqrt{(3 + \kappa)(1 + 3\kappa)} > 1 - \kappa^2$  and a right linear tail, i.e.  $\lambda_+ < \tilde{\lambda}_+$ , for  $\kappa > 1$  [66]. Fig. 2 reports the phase diagrams of the system as deduced by inspecting the ratios  $r_- \equiv \lambda_- / \tilde{\lambda}_-$  and  $r_+ \equiv \lambda_+ / \tilde{\lambda}_+$ . Figs. 2(a) and 2(b) show that at stationarity and at large  $\kappa$  and  $\text{Pe}$  the effective domain is significantly smaller than the primary domain with  $\lambda_- \gg \tilde{\lambda}_-$  or  $\lambda_+ \ll \tilde{\lambda}_+$ , respectively. Fig. 2(c) and Fig. 2(d) depict  $r_-$  and  $r_+$  under non-stationary initial conditions for fixed values of  $\kappa$  and  $\text{Pe}$  such that the corresponding stationary problem has no linear tail. The

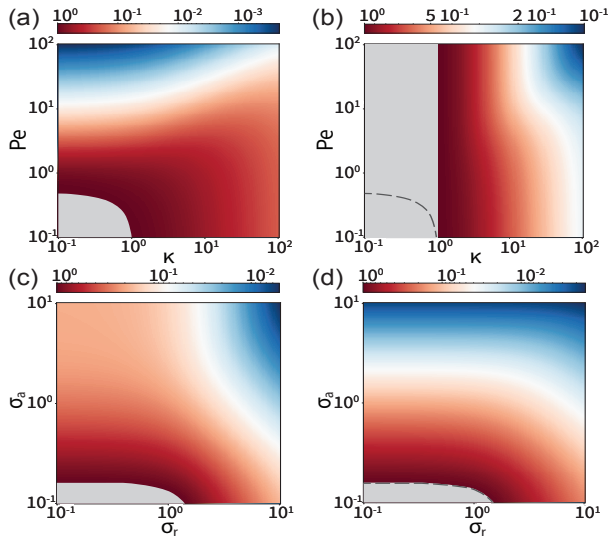


FIG. 2. Phase diagram as deduced by the ratios  $r_- \equiv \lambda_-/\tilde{\lambda}_-$  and  $r_+ \equiv \lambda_+/\tilde{\lambda}_+$  between the effective and primary domain boundary points of the asymptotic cumulant generating function. Colored areas denote regions where a dynamical phase transition occurs, i.e.  $r_- < 1$  or  $r_+ < 1$ , and the color scale measures  $r_-$  and  $r_+$ . Gray areas denote regions without a singularity, i.e.  $r_- = 1$  or  $r_+ = 1$ . (a) and (b):  $r_-$  and  $r_+$  under the stationary initial condition in the  $\kappa$ -Pe plane. (c) and (d):  $r_-$  and  $r_+$  under the non-stationary initial condition in the  $\sigma_r$ - $\sigma_a$  plane at  $\kappa = 0.7$  and  $Pe = 0.1$  for which there is no dynamical phase transition at stationarity. The regions under the dashed lines do not exhibit any phase transition.

effective domain is significantly smaller than the primary domain with  $\lambda_- \gg \tilde{\lambda}_-$  or  $\lambda_+ \ll \tilde{\lambda}_+$  at large  $\sigma_r$  and  $\sigma_a$ . We note that the results of Ref. [60] on the free AOUP are consistently recovered in the limit  $\kappa \downarrow 0$  by the confined non-stationary model with  $\sigma_a = Pe$  [66]. Singularities of the rate function are lost in this limit.

Interpretation of the singularities of the rate function requires to analyze the particle trajectories. Fig. 3(a) reports three typical trajectories at stationarity with large  $\kappa$  and  $Pe$  conditional on  $W_\tau = w\tau$  with  $w \ll w_-$  in the far left linear tail,  $w \approx \langle w \rangle$ , and  $w \gg w_+$  in the far right linear tail.  $\langle w \rangle$  is the typical value of the active work, that is  $I(\langle w \rangle) = 0$ . A large fluctuation  $w \ll w_-$  of the active work involves a short initial transient during which the particle is captured by the harmonic trap. Fig. 3(b) shows that this transient is characterized by a large value of the initial position,  $r(0) \sim \sqrt{\tau}$ , which goes along with a large value of the initial active force,  $a(0) \sim \sqrt{\tau}$ , in the same direction since  $r(0)$  and  $a(0)$  are positively correlated by Eq. (2). The contribution of these large values to the active work is of order  $-a(0)r(0) \sim \tau$  and negative because the particle moves oppositely to the active force. In conclusion, the most likely way to realize the rare event  $w \ll w_-$  is that an initial transient provides a macroscopic fraction of the large fluctuation, with the active force trying to push the particle out of the harmonic trap unsuccessfully. Specularly, a large fluctuation  $w \gg w_+$  entails a final short transient during which the

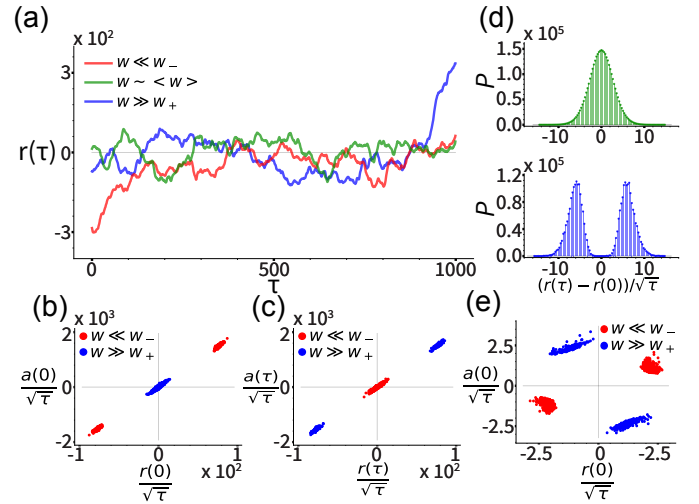


FIG. 3. Trajectory analysis at stationarity with  $\kappa = 20.0$  and  $Pe = 200.0$  and under the non-stationary initial condition with  $\kappa = 0.7$  and  $Pe = 0.1$ . (a): typical trajectories of the particle in the stationary configuration up to time  $\tau = 10^3$  corresponding to  $w = 26 \ll w_- = 1.73 \cdot 10^3$  (red),  $w = 1.92 \cdot 10^3 \approx \langle w \rangle$  (green), and  $w = 4.10 \cdot 10^3 \gg w_+ = 2.11 \cdot 10^3$  (blue). (b) and (c): initial and ending points of a pool of stationary trajectories corresponding to  $w \leq 8.00 \cdot 10^2 \ll w_-$  and  $w \geq 3.20 \cdot 10^3 \gg w_+$ , respectively. (d): stationary probability distribution of the particle's net displacement conditional on typical  $w$  in the interval  $-\sigma_w < w - \langle w \rangle < \sigma_w$  (top) and on large  $w$  in the interval  $3\sigma_w < w - \langle w \rangle < 4\sigma_w$  (bottom),  $\sigma_w$  being the standard deviation of the active work taking value  $\sigma_w \sim 2.76 \cdot 10^2$  at  $\tau = 10^3$ . (e): initial and ending points of a pool of non-stationary trajectories with  $\sigma_r = \sigma_a = 10$  and  $\tau = 2 \cdot 10^4$  corresponding to  $w \leq -5.00 \cdot 10^{-2} \ll w_- = 1.09 \cdot 10^{-3}$  and  $w \geq 2.50 \cdot 10^{-1} \gg w_+ = 8.19 \cdot 10^{-2}$ , respectively.

particle escapes from the trap. In fact, Fig. 3(c) proves that there are large final values of the position and the active force,  $r(\tau) \sim \sqrt{\tau}$  and  $a(\tau) \sim \sqrt{\tau}$ , and that they are in the same direction. This time the active force successfully pushes the particle out of the harmonic trap, so that the contribution of these large values to the active work is positive and of order  $a(\tau)r(\tau) \sim \tau$ . None of the above transients is observed when  $w \approx \langle w \rangle$ . According to Fig. 3(d), the distribution of the net displacement of the particle in a time interval  $\tau$  has only one peak at zero when  $w \approx \langle w \rangle$  and two symmetric peaks due to final large values when  $w \gg w_+$ .

Finally, under the non-stationary initial condition with small  $\kappa$  and  $Pe$ , where dynamical phase transitions do not occur at stationarity, we observe singularities at both  $w \ll w_-$  and  $w \gg w_+$ . These singularities arise solely due to large values in the initial condition,  $r(0) \sim \sqrt{\tau}$  and  $a(0) \sim \sqrt{\tau}$  as shown by Fig. 3(e), with the particle captured by the harmonic trap providing a contribution of order  $-a(0)r(0) \sim \tau$  to the active work. The latter can be either negative or positive since  $r(0)$  and  $a(0)$  are now uncorrelated.

The occurrence of a large deviation of the active work due to large values of either  $r(0)$  and  $a(0)$  or  $r(\tau)$  and  $a(\tau)$



is reminiscent of some big-jump phenomena observed in sums of independent random variables [19, 21, 26, 69]. The latter works have understood that a fluctuation in the linear tail of the rate function can be decomposed in two parts: many small deviations in the same direction which sum up to the singular point, and a big jump of a single variable summing to the actual value of the fluctuation. Basically, we find that a large fluctuation of the active work is realized in a similar way through some localized big jumps. At variance with sums of independent random variables where summands are exchangeable, here the structure of the process imposes that the big jumps localize at the initial or at the ending points of the trajectories. In fact,  $r(t)$  and  $a(t)$  are always positively correlated. Thus, suppose a big jump of  $r(t)$  and  $a(t)$  occurs at an intermediate time  $t$ , with the particle escaping the potential up to  $t$  and generating a certain positive active work; afterwards, the particle is bound to be recatched by the potential, and in doing so generates a negative active work that cancels out the first contribution.

In summary, we have characterized the active work large fluctuations of an active Ornstein-Uhlenbeck particle under the action of a harmonic potential. We have demonstrated that harmonic confinement can induce dynamical phase transitions at sufficiently large active and harmonic force parameters. Furthermore, we have provided an in-depth understanding of the origin of these transitions in terms of phase separation in trajectory space driven by big-jump mechanisms. These results can contribute to understand the origin of singularities in active work rate functions in more complex systems of interacting active Brownian particles. We argue that our approach can be extended to the study of fluctuations in systems of several Ornstein-Uhlenbeck particles coupled via elastic forces, like active polymers.

This work has been supported by the Italian Ministry of University and Research via the project PRIN/2020 PFCXPE and by Apulia Region via the project UNIBA044 of the research programme REFIN - Research for Innovation.

---

[1] R. Ellis, *Entropy, Large Deviations, and Statistical Mechanics* (Springer New York, 1985).  
 [2] H. Touchette, *Phys. Rep.* **478**, 1 (2009).  
 [3] A. Dembo and O. Zeitouni, *Large Deviations Techniques and Applications*, 2nd ed. (Springer - New York, 1988).  
 [4] F. den Hollander, *Large Deviations* (AMS, 2000).  
 [5] R. L. Jack, *Eur Phys J B* **93**, 1 (2020).  
 [6] T. Bodineau and B. Derrida, *Phys. Rev. E* **72**, 066110 (2005).  
 [7] R. J. Harris, A. Rákos, and G. M. Schütz, *J. Stat. Mech. Theory Exp.* **2005**, P08003 (2005).  
 [8] P. Visco, *J. Stat. Mech. Theory Exp.* **2006**, P06006 (2006).

[9] J. Mehl, T. Speck, and U. Seifert, *Phys. Rev. E* **78**, 011123 (2008).  
 [10] P. I. Hurtado and P. L. Garrido, *Phys. Rev. Lett.* **107**, 180601 (2011).  
 [11] L. Bertini, A. De Sole, D. Gabrielli, G. Jona-Lasinio, and C. Landim, *J. Stat. Mech. Theory Exp.* **2010**, L11001 (2010).  
 [12] M. Lefevere, R. Mariani and L. Zambotti, *J Math Phys* **52**, 033302 (2011).  
 [13] G. Bunin, Y. Kafri, and D. Podolsky, *EPL* **99**, 20002 (2012).  
 [14] T. Speck, A. Engel, and U. Seifert, *J. Stat. Mech. Theory Exp.* **2012**, P12001 (2012).  
 [15] T. R. Gingrich, S. Vaikuntanathan, and P. L. Geissler, *Phys. Rev. E* **90**, 042123 (2014).  
 [16] P. T. Nyawo and H. Touchette, *EPL* **116**, 50009 (2016).  
 [17] R. J. Harris and H. Touchette, *J. Phys. A Math. Theor.* **50**, 10LT01 (2017).  
 [18] M. Zamparo, *J. Phys. A Math. Theor.* **52**, 495004 (2019).  
 [19] I. Jeon, P. March, and B. Pittel, *Ann Probab* **28**, 1162 (2000).  
 [20] S. N. Majumdar, M. R. Evans, and R. K. P. Zia, *Phys. Rev. Lett.* **94**, 180601 (2005).  
 [21] I. Armendáriz and M. Loulakis, *Probab Theory Relat Fields* **145**, 175 (2009).  
 [22] N. Merhav and Y. Kafri, *J. Stat. Mech. Theory Exp.* **2010**, P02011 (2010).  
 [23] J. Szavits-Nossan, M. R. Evans, and S. N. Majumdar, *Phys. Rev. Lett.* **112**, 020602 (2014).  
 [24] F. Corberi, G. Gonnella, A. Piscitelli, and M. Zannetti, *J. Phys. A Math. Theor.* **46**, 042001 (2013).  
 [25] M. Zannetti, *EPL* **111**, 20004 (2015).  
 [26] C. Godréche, *J. Stat. Mech. Theory Exp.* **2019**, 063207 (2019).  
 [27] M. Zamparo, *J. Phys. A Math. Theor.* **55**, 484001 (2022).  
 [28] J. P. Garrahan, R. L. Jack, V. Lecomte, E. Pitard, K. van Duijvendijk, and F. van Wijland, *J. Phys. A Math. Theor.* **42**, 075007 (2009).  
 [29] R. L. Jack and P. Sollich, *Prog. Theor. Phys. Supplement* **184**, 304 (2010).  
 [30] J. Tailleur and J. Kurchan, *Nat. Phys.* **3**, 203 (2007).  
 [31] G. Gompper *et al.*, *J. Phys. Condens. Matter* **32**, 193001 (2020).  
 [32] J. Tailleur and M. E. Cates, *Phys. Rev. Lett.* **100**, 218103 (2008).  
 [33] P. Pietzonka, K. Kleinbeck, and U. Seifert, *New J. Phys.* **18**, 052001 (2016).  
 [34] F. Cagnetta, F. Corberi, G. Gonnella, and A. Suma, *Phys. Rev. Lett.* **119**, 158002 (2017).  
 [35] S. Whitelam, K. Klymko, and D. Mandal, *J. Chem. Phys.* **148**, 154902 (2018).  
 [36] T. GrandPre and D. T. Limmer, *Phys. Rev. E* **98**, 060601 (2018).  
 [37] G. Gradenigo and S. N. Majumdar, *J. Stat. Mech. Theory Exp.* **2019**, 053206 (2019).  
 [38] F. Cagnetta and E. Mallmin, *Phys. Rev. E* **101**, 022130 (2020).  
 [39] E. Fodor, T. Nemoto, and S. Vaikuntanathan, *New J. Phys.* **22**, 013052 (2020).  
 [40] D. C. and A. D., *Journal of Statistical Mechanics: Theory and Experiment* **2021**, 013207 (2021).  
 [41] T. GrandPre, K. Klymko, K. K. Mandadapu, and D. T. Limmer, *Phys. Rev. E* **103**, 012613 (2021).  
 [42] N. R. Smith and O. Farago, *Phys. Rev. E* **106**, 054118

- (2022).
- [43] T. Nemoto, E. Fodor, M. E. Cates, R. L. Jack, and J. Tailleur, *Phys. Rev. E* **99**, 022605 (2019).
- [44] Y.-E. Keta, E. Fodor, F. van Wijland, M. E. Cates, and R. L. Jack, *Phys. Rev. E* **103**, 022603 (2021).
- [45] T. Agranov, M. E. Cates, and R. L. Jack, *J. Stat. Mech. Theory Exp.* **2022**, 123201 (2022).
- [46] N. Kumar, S. Ramaswamy, and A. K. Sood, *Phys. Rev. Lett.* **106**, 118001 (2011).
- [47] G. Gradenigo, A. Sarracino, A. Puglisi, and H. Touchette, *J. Phys. A Math. Theor.* **46**, 335002 (2013).
- [48] G. Szamel, *Phys. Rev. E* **90**, 012111 (2014).
- [49] C. Maggi, U. M. B. Marconi, N. Gnan, and R. Di Leonardo, *Sci. Rep.* **5**, 10742 (2015).
- [50] T. F. F. Farage, P. Krinninger, and J. M. Brader, *Phys. Rev. E* **91**, 042310 (2015).
- [51] E. Fodor, C. Nardini, M. E. Cates, J. Tailleur, P. Visco, and F. van Wijland, *Phys. Rev. Lett.* **117**, 038103 (2016).
- [52] L. Caprini, U. M. B. Marconi, A. Puglisi, and A. Vulpiani, *J. Chem. Phys.* **150**, 024902 (2019).
- [53] D. Martin, J. O’Byrne, M. E. Cates, E. Fodor, C. Nardini, J. Tailleur, and F. van Wijland, *Phys. Rev. E* **103**, 032607 (2021).
- [54] A. Crisanti and M. Paoluzzi, [arXiv:2212.05941](https://arxiv.org/abs/2212.05941) (2022).
- [55] M. Caraglio and T. Franosch, *Phys. Rev. Lett.* **129**, 158001 (2022).
- [56] N. Arsha, K. P. Jepsin, and M. Sahoo, [arXiv:2208.14443](https://arxiv.org/abs/2208.14443) (2022).
- [57] G. Szamel, [arXiv:2211.15714](https://arxiv.org/abs/2211.15714) (2022).
- [58] S. K. Nandi and N. S. Gov, *Soft Matter* **13**, 7609 (2017).
- [59] E. Woillez, Y. Kafri, and N. S. Gov, *Phys. Rev. Lett.* **124**, 118002 (2020).
- [60] M. Semeraro, A. Suma, I. Petrelli, F. Cagnetta, and G. Gonnella, *J. Stat. Mech. Theory Exp.* **2021**, 123202 (2021).
- [61] S. Das, G. Gompper, and R. G. Winkler, *New J. Phys.* **20**, 015001 (2018).
- [62] S. Mandal, B. Liebchen, and H. Löwen, *Phys. Rev. Lett.* **123**, 228001 (2019).
- [63] The results we present here are based on the Stratonovich prescription. We have checked that the Itô definition leads to the same findings.
- [64] L. Onsager and S. Machlup, *Phys. Rev.* **91**, 1505 (1953).
- [65] C. W. Gardiner, *Handbook of Stochastic Methods*, 3rd ed. (Springer - New York, 2003).
- [66] See Supplemental Material for additional information.
- [67] M. Zamparo and M. Semeraro, *J. Math. Phys.* **64**, 023302 (2023).
- [68] J. Gutierrez-Gutierrez and P. M. Crespo, *IEEE Trans. Inf. Theory* **54**, 5671 (2008).
- [69] M. R. Evans, S. N. Majumdar, and R. K. P. Zia, *J Stat Phys* **123**, 357 (2006).